Available online at www.sciencedirect.com

SCIENCE DIRECT®

International Journal of Heat and Mass Transfer 47 (2004) 2567–2576

International Journal of HEAT and MASS TRANSFER

www.elsevier.com/locate/ijhmt

Group preserving scheme for backward heat conduction problems

Chein-Shan Liu *

Department of Mechanical and Marine Engineering, Taiwan Ocean University, Keelung 202-24, Taiwan

Received 27 November 2003; received in revised form 22 December 2003

Abstract

In this paper we numerically integrate the backward heat conduction equation $\partial u/\partial t = \nu \triangle u$, in which the Dirichlet boundary conditions are specified at the boundary of a certain spatial domain and a final data is specified at time $T > 0$. In order to treat this ill-posed problem we first convert it through the transformation $s = T - t$ to an unstable initial-boundary-value problem: $\partial u/\partial s = -\nu \triangle u$ together with the same boundary conditions and the same data at $s = 0$. Then, we consider the contraction map of u to $v = \exp[-as]u$ by a suitable contraction factor $a > 0$, which is analyzed by considering the stability of the semi-discretization numerical schemes. The resulting ordinary differential equations at the interior grid points are then numerically integrated by the group preserving scheme, proposed by Liu [Int. J. Non-Linear Mech. 36 (2001) 1047], and the stable range of the index $r = \nu \Delta t/(\Delta x)^2$ is derived. Numerical tests for both forward and backward heat conduction problems are performed to confirm the effectiveness of the new numerical methods.

Keywords: Backward heat conduction problem; Group preserving scheme; Semi-discretization

1. Introduction

The heat conduction problem we consider is:

$$\frac{\partial u}{\partial t} = \nu \triangle u \quad \text{in } \Omega, \tag{1}$$

$$u = u_B \quad \text{on } \Gamma_B, \tag{2}$$

$$u = u_F \quad \text{on } \Gamma_F, \tag{3}$$

where u is a scalar temperature field of heat distribution and ν is the heat diffusion coefficient. We take a bounded domain D in $\mathbb{R}^k$ and a spacetime domain $\Omega = D \times (0, T)$ in $\mathbb{R}^{k+1}$ for a final time $T > 0$, and write two surfaces $\Gamma_B = \partial D \times [0, T]$ and $\Gamma_F = D \times \{T\}$ of the boundary $\partial\Omega$. $\triangle$ denotes the k-dimensional Laplacian operator. Eqs. (1)–(3) constitute a k-dimensional backward heat conduction problem for a given boundary data $u_B : \Gamma_B \mapsto \mathbb{R}$ and a final data $u_F : \Gamma_F \mapsto \mathbb{R}$.

The backward heat conduction problem is an ill-posed problem [1] in the sense that the solution is unstable for a given final data u_F. For example, $u(x, t) = \exp[\alpha^2(T - t)] \sin \alpha x$ is the solution of Eq. (1) with $k = 1$ and $\nu = 1$, subjecting to the final data $u(x, T) = \sin \alpha x$. Thus, by taking α arbitrarily large $u(x, 0) = \exp[\alpha^2 T] \sin \alpha x$ can become unbounded.

It is well known that the approach of ill-posed problems by numerical methods is usually difficult [2–7]. For example, for any time step size $\Delta t > 0$ in the time range $[0, T]$, and for any lattice spacing length $\Delta x_1 > 0, \ldots, \Delta x_k > 0$, in each coordinate we can show that the following finite-difference scheme of Eq. (1) is unstable even under the von Neumann condition, which is a necessary numerical stability condition for the forward finite difference scheme of initial-value problem [8]:

* Tel.: +886-2-2462-2192x3252; fax: +886-2-2462-0836.
E-mail address: csilu@mail.notu.edu.tw (C.-S. Liu).

0017-9310/$ - see front matter © 2004 Elsevier Ltd. All rights reserved.
doi:10.1016/j.ijheatmasstransfer.2003.12.019

Nomenclature

a	contraction factor
b	$=\frac{a(\Delta x)^2}{\nu}$: constant
$\mathbf{A}$	augmented matrix
$\mathbf{A}_j$	coefficient matrix at the jth time step
C	constant
$\mathbf{C}$	constant matrix
D	domain in $\mathbb{R}^k$
∂D	the boundary of D
$\mathbb{D}$	domain in $\mathbb{R}^n \times \mathbb{R}$
$\mathbf{f}$	n-dimensional vector field
$\mathbf{f}^j$	numerical value of $\mathbf{f}$ at the jth time step
$\mathbf{g}$	$n+1$-dimensional Minkowski metric
$\mathbf{I}_n$	n-dimensional unit matrix
$\mathscr{L}$	Lipschitz constant
$\Vert \bullet \Vert$	Euclidean norm
$\Vert \bullet \Vert_{L^2}$	L^2-norm
m	index $m = 1, \dots, n$
$\mathbb{M}^{n+1}$	$n+1$-dimensional Minkowski space
$\mathbf{n}^j$	unit vector at the jth time step
n	number of interior grid points
n_s	number of reverse time steps
n_t	number of time steps
$\mathbb{N}$	the set of positive integers
$O(1)$	order of numerical value
r	$=\frac{\nu\Delta t}{(\Delta x)^2}$: stability index
$r_{\max}$	maximum value of r for stability
$\mathbb{R}$	the set of real numbers
$\mathbb{R}^n$	n-dimensional real space
s	$= T - t$: reverse time
Δs	reverse time increment
$SO_o(n,1)$	$n+1$-dimensional Lorentz group
t	time
t_j	discretized time of jth step
Δt	time increment
T	final time
$[0,T]$	the times t such that $0 \leqslant t \leqslant T$
$(0,T)$	the times t such that $0 < t < T$
u	heat distribution
u_i	numerical value of u at the ith grid point
u_i^j	the jth time step value of u at the ith grid point
$u_{i,j}$	numerical value of u at the (i,j)th grid point
$v_{i,j}$	numerical value of v at the (i,j)th grid point
$\mathbf{u}$	n-dimensional vector
$\mathbf{u}^j$	numerical value of $\mathbf{u}$ at the jth time step
u_B	the boundary value on Γ_B
u_F	the final data on Γ_F
$\mathbf{v}^j$	numerical value of $\mathbf{v}$ at the jth reverse time step
v	$= \exp[-as]u$: new variable
x	space variable
Δx	lattice spacing length of x
x_k	the kth space coordinate
Δx_k	lattice spacing length of x_k
$\mathbf{X}$	$n+1$-dimensional augmented vector
y	space variable
Δy	lattice spacing length of y

Greek symbols

α	constant
η_j	adaptive factor at the jth time step
Ω	$= D \times (0,T)$: spacetime domain
$\partial\Omega$	the boundary of Ω
Γ_B	$= \partial D \times [0,T]$: t-direction boundary of Ω
Γ_F	$= D \times \{T\}$: final time boundary of Ω
$\triangle$	Laplace operator
ν	heat diffusion coefficient

Subscripts and superscripts

i,j,k	indices
t	transpose

$$\begin{aligned}\frac{u(x_1,\dots,x_k,t+\Delta t)-u(x_1,\dots,x_k,t)}{\nu\Delta t} &= \{u(x_1+\Delta x_1,\dots,x_k,t)-2u(x_1,\dots,x_k,t)\\ &\quad + u(x_1-\Delta x_1,\dots,x_k,t)\}/(\Delta x_1)^2+\cdots\\ &\quad + \{u(x_1,\dots,x_k+\Delta x_k,t)-2u(x_1,\dots,x_k,t)\\ &\quad + u(x_1,\dots,x_k-\Delta x_k,t)\}/(\Delta x_k)^2. \end{aligned} \tag{4}$$

In order to calculate the backward heat conduction problems, there appears certain progress in this issue, including, for example, the boundary element method [2], the iterative boundary element method [3,4], the operator-splitting method [5], and the lattice-free high-order finite difference method [6]. A recent review of the numerical backward heat conduction problems was provided in [7]. In this paper we are going to calculate the heat conduction problems (forward or backward) by a semi-discretization method, which replaces Eq. (4) by a set of ordinary differential equations:

$$\begin{aligned}\frac{\partial u(x_1,\dots,x_k,t)}{\nu\partial t} &= \{u(x_1+\Delta x_1,\dots,x_k,t)-2u(x_1,\dots,x_k,t)\\ &\quad + u(x_1-\Delta x_1,\dots,x_k,t)\}/(\Delta x_1)^2+\cdots\\ &\quad + \{u(x_1,\dots,x_k+\Delta x_k,t)-2u(x_1,\dots,x_k,t)\\ &\quad + u(x_1,\dots,x_k-\Delta x_k,t)\}/(\Delta x_k)^2 \end{aligned} \tag{5}$$

At the interior grid points we select in the domain D, together with the group preserving scheme for ordinary differential equations developed in [9].

Consider a system of n ordinary differential equations:

$$\dot{\mathbf{u}} = \mathbf{f}(\mathbf{u}, t), \quad \mathbf{u} \in \mathbb{R}^n, \quad t \in \mathbb{R}, \tag{6}$$

where $\mathbf{u}$ is an n-dimensional vector, t is a time variable, and $\mathbf{f}$ is a vector-valued function of $\mathbf{u}$ and t, also named vector field. The dot stands for the differential with respect to t. For the uniqueness of the solution, the Lipschitz condition is assumed:

$$\|\mathbf{f}(\mathbf{u}, t) - \mathbf{f}(\mathbf{y}, t)\| \leqslant \mathscr{L}\|\mathbf{u} - \mathbf{y}\|, \quad \forall(\mathbf{u}, t), (\mathbf{y}, t) \in \mathbb{D}, \tag{7}$$

where $\mathbb{D}$ is a domain in $\mathbb{R}^n \times \mathbb{R}$, and $\mathscr{L}$ is known as a Lipschitz constant.

Liu [9] has extended Eq. (6) to the following form:

$$\frac{\mathrm{d}}{\mathrm{d}t}\begin{bmatrix} \mathbf{u} \\ \|\mathbf{u}\| \end{bmatrix} = \begin{bmatrix} \mathbf{0}_{n\times n} & \frac{\mathbf{f}(\mathbf{u},t)}{\|\mathbf{u}\|} \\ \frac{\mathbf{f}^{\mathrm{t}}(\mathbf{u},t)}{\|\mathbf{u}\|} & 0 \end{bmatrix}\begin{bmatrix} \mathbf{u} \\ \|\mathbf{u}\| \end{bmatrix} \tag{8}$$

if $\|\mathbf{u}\| > 0$, where $\|\mathbf{u}\|$ stands for the Euclidean norm of $\mathbf{u}$, and the superscript 't' denotes the transpose. It is obvious that the first equation is the same as the original equation (6), but the introduction of the second equation led to a Minkowskian structure for the augmented non-linear system with the augmented variables $\mathbf{X} = (\mathbf{u}^{\mathrm{t}}, \|\mathbf{u}\|)^{\mathrm{t}}$ satisfying

$$\mathbf{X}^{\mathrm{t}}\mathbf{g}\mathbf{X} = 0, \tag{9}$$

where

$$\mathbf{g} = \begin{bmatrix} \mathbf{I}_n & \mathbf{0}_{n\times 1} \\ \mathbf{0}_{1\times n} & -1 \end{bmatrix} \tag{10}$$

is a Minkowski metric, and $\mathbf{I}_n$ is the identity matrix of order n.

For this form $\dot{\mathbf{X}} = \mathbf{A}\mathbf{X}$ the augmented matrix $\mathbf{A}$ is given by

$$\mathbf{A} = \begin{bmatrix} \mathbf{0}_{n\times n} & \frac{\mathbf{f}(\mathbf{u},t)}{\|\mathbf{u}\|} \\ \frac{\mathbf{f}^{\mathrm{t}}(\mathbf{u},t)}{\|\mathbf{u}\|} & 0 \end{bmatrix}, \tag{11}$$

and satisfies

$$\mathbf{A}^{\mathrm{t}}\mathbf{g} + \mathbf{g}\mathbf{A} = \mathbf{0}, \tag{12}$$

which shows that $\mathbf{A}$ is a Lie algebra of the Lorentz group $\mathrm{SO}_o(n, 1)$.

2. The group preserving schemes

Remarkably the original n-dimensional dynamical system (6) in $\mathbb{R}^n$ can be embedded naturally into an augmented $n+1$-dimensional dynamical system (8) in $\mathbb{M}^{n+1}$, satisfying the cone condition:

$$\mathbf{X}^{\mathrm{t}}\mathbf{g}\mathbf{X} = \mathbf{u}\cdot\mathbf{u} - \|\mathbf{u}\|^2 = \|\mathbf{u}\|^2 - \|\mathbf{u}\|^2 = 0, \tag{13}$$

which is thus the most natural constraint that we can impose on the dynamical system (8). Even raising the dimension of the new system by one, shows that the new system with its Lie algebra property (12) has the advantage of allowing us to develop the group preserving numerical scheme [9]:

$$\mathbf{u}^{j+1} = \mathbf{u}^j + \frac{4\Delta t\|\mathbf{u}^j\|^2 + 2(\Delta t)^2\mathbf{f}^j\cdot\mathbf{u}^j}{4\|\mathbf{u}^j\|^2 - (\Delta t)^2\|\mathbf{f}^j\|^2}\mathbf{f}^j. \tag{14}$$

The numerical formula (14), which upon comparing with the Euler scheme

$$\mathbf{u}^{j+1} = \mathbf{u}^j + \Delta t\mathbf{f}^j,$$

can be viewed as a weighting factor adaptive numerical scheme:

$$\mathbf{u}^{j+1} = \mathbf{u}^j + \eta_j\Delta t\mathbf{f}^j \tag{15}$$

with the adaptive factor

$$\eta_j = \frac{4\|\mathbf{u}^j\|^2 + 2\Delta t\mathbf{f}^j\cdot\mathbf{u}^j}{4\|\mathbf{u}^j\|^2 - (\Delta t)^2\|\mathbf{f}^j\|^2} \tag{16}$$

changing step-by-step. In above, $\mathbf{u}^j$ denotes the numerical value of $\mathbf{u}$ at a discrete time t_j, $\Delta t = t_{j+1} - t_j$ is a uniform time increment, and $\mathbf{f}^j$ denotes $\mathbf{f}(\mathbf{u}^j, t_j)$.

3. The forward heat conduction problems

3.1. Semi-discretization

The numerical method of line is simple in concept, that for a given system of partial differential equations discretize all but one of the independent variables [10]. The semi-discrete procedure yields a coupled system of ordinary differential equations, which are then numerically integrated. For the one-dimensional heat flow equation we adopt the numerical method of line to discretize the spatial coordinate x by

$$\left.\frac{\partial^2 u(x,t)}{\partial x^2}\right|_{x=i\Delta x} = \frac{u_{i+1}(t) - 2u_i(t) + u_{i-1}(t)}{(\Delta x)^2},$$

where Δx is a uniform discretization spacing length, and $u_i(t) = u(i\Delta x, t)$, such that Eq. (1) can be approximated by

$$\frac{\partial u_i(t)}{\partial t} = \frac{v}{(\Delta x)^2}[u_{i+1}(t) - 2u_i(t) + u_{i-1}(t)]. \tag{17}$$

The next step is to advance the solution from the initial condition to the desired time T. Really, Eq. (17) has totally n coupled linear differential equations for the n variables $u_i(t), i = 1, 2, \ldots, n$, which can be numerically integrated to obtain the solutions. If we further assume that

$$\frac{\partial u_i(t)}{\partial t} = \frac{u_i((j+1)\Delta t) - u_i(j\Delta t)}{\Delta t}$$

by a forward time difference for the partial derivative of u with respect to t, then we fully discretize Eq. (1) into the following form:

$$u_i^{j+1} = r[u_{i+1}^j + u_{i-1}^j] + (1-2r)u_i^j,\quad j = 0,1,\ldots,n_t,\ \ i = 1,\ldots,n, \tag{18}$$

where n_t is the number of time steps such that $\Delta t = T/n_t$, and all $u_i^0, i = 1,\ldots,n$, are known from the initial condition. For saving notation we have let

$$u_i^j = u(i\Delta x, j\Delta t), \tag{19}$$

and

$$r = \frac{\nu \Delta t}{(\Delta x)^2} \tag{20}$$

denote the stability index. We can step the solution u_i^{j+1} forward in time according to Eq. (18), since all the terms on the right-hand side are already known at the previous time step. If the ratio r is chosen as less than one-half, there will be improved accuracy. If the ratio r is chosen greater than one-half, the number of calculations required to advance the solution through a given interval of time would reduce. However, for numerical scheme (18) there is no such freedom to select larger r, because when $r > 1/2$ the instability renders the scheme to fail to calculate the heat responses [8].

3.2. Group preserving scheme

In addition to the explicit scheme of the Euler type, introduced in the previous subsection, we attempt to develop another explicit scheme for the heat flow equation according to the formalism specified in Section 2. From Eq. (17) we have an ordinary differential equations system for the n unknowns $u_i(t), i = 1,2,\ldots,n$. Employing the numerical scheme developed in Section 2 to Eq. (17) we obtain

$$u_i^{j+1} = u_i^j + \eta_j r[u_{i+1}^j - 2u_i^j + u_{i-1}^j], \tag{21}$$

which is then rearranged to

$$u_i^{j+1} = r\eta_j[u_{i+1}^j + u_{i-1}^j] + (1-2r\eta_j)u_i^j. \tag{22}$$

If $\eta_j = 1$ for each time step t_j, then the above scheme is reduced to scheme (18).

3.3. Stability analysis

Let us introduce the constant matrix

$$\mathbf{C} = \begin{bmatrix} -2 & 1 & & & \\ 1 & -2 & 1 & & \\ & \cdot & \cdot & \cdot & \\ & & \cdot & \cdot & \cdot \\ & & & \cdot & \cdot & \cdot \\ & & & & 1 & -2 \end{bmatrix}, \tag{23}$$

whose dimension is $n \times n$. The factor η_j in Eq. (21) can be written as

$$\eta_j = \frac{4\|\mathbf{u}^j\|^2 + 2r(\mathbf{u}^j)^{\mathrm{t}}\mathbf{C}\mathbf{u}^j}{4\|\mathbf{u}^j\|^2 - r^2(\mathbf{u}^j)^{\mathrm{t}}\mathbf{C}^2\mathbf{u}^j}, \tag{24}$$

upon inserting the vector fields $\mathbf{f}^j = \nu\mathbf{C}\mathbf{u}^j/(\Delta x)^2$ into Eq. (16), where $\mathbf{u}^j = (u_1^j, u_2^j, \ldots, u_n^j)^{\mathrm{t}}$. The eigenvalues of $\mathbf{C}$ are found to be

$$-4\sin^2\frac{m\pi}{2(n+1)},\quad m = 1,2,\ldots,n, \tag{25}$$

which together with the symmetry of $\mathbf{C}$ indicates that $\mathbf{C}$ is negative definite. Thus, from Eq. (24) it follows that

$$\eta_j = \frac{4 - 2r(\mathbf{n}^j)^{\mathrm{t}}(-\mathbf{C})\mathbf{n}^j}{4 - r^2(\mathbf{n}^j)^{\mathrm{t}}\mathbf{C}^2\mathbf{n}^j}, \tag{26}$$

where $\mathbf{n}^j = \mathbf{u}^j/\|\mathbf{u}^j\|$ is a unit vector. Because of

$$4\sin^2\frac{n\pi}{2(n+1)} \geqslant (\mathbf{n}^j)^{\mathrm{t}}(-\mathbf{C})\mathbf{n}^j \geqslant 4\sin^2\frac{\pi}{2(n+1)}, \tag{27}$$

$$16\sin^4\frac{n\pi}{2(n+1)} \geqslant (\mathbf{n}^j)^{\mathrm{t}}\mathbf{C}^2\mathbf{n}^j \geqslant 16\sin^4\frac{\pi}{2(n+1)}, \tag{28}$$

the upper bound of η_j can be estimated as follows:

$$\eta_j \leqslant \frac{1 - 2r\sin^2\frac{\pi}{2(n+1)}}{1 - 4r^2\sin^4\frac{n\pi}{2(n+1)}}. \tag{29}$$

We proceed to investigate the stability of scheme (22), which can be expressed as the matrix equation

$$\begin{bmatrix} u_1^{j+1} \\ u_2^{j+1} \\ \cdot \\ \cdot \\ \cdot \\ u_n^{j+1} \end{bmatrix} = \begin{bmatrix} 1-2\eta_j r & \eta_j r & & & \\ \eta_j r & 1-2\eta_j r & \eta_j r & & \\ & \cdot & \cdot & \cdot & \\ & & \cdot & \cdot & \cdot \\ & & & \cdot & \cdot & \cdot \\ & & & & \eta_j r & 1-2\eta_j r \end{bmatrix} \begin{bmatrix} u_1^j \\ u_2^j \\ \cdot \\ \cdot \\ \cdot \\ u_n^j \end{bmatrix}, \tag{30}$$

or in vector form

$$\mathbf{u}^{j+1} = \mathbf{A}_j\mathbf{u}^j = (\mathbf{I}_n + \eta_j r\mathbf{C})\mathbf{u}^j, \tag{31}$$

where $\mathbf{A}_j$ represents the coefficient matrix at the time step t_j. The eigenvalues of $\mathbf{A}_j$ are found to be

$$1 - 4\eta_j r\sin^2\frac{m\pi}{2(n+1)},\quad m = 1,2,\ldots,n.$$

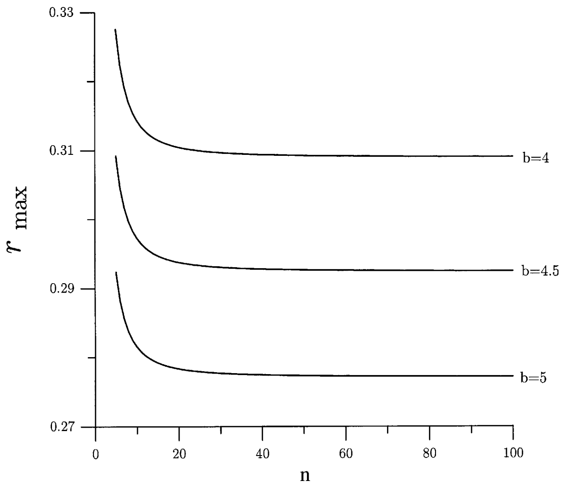

Fig. 1. The sufficient condition of the stability of the group preserving scheme is obtained by $r < r_{\max}$, which is plotted with respect to the number n of the interior grid points. For the backward problem it shares the same curve if $b = 4$.

Thus, we have a stable scheme for Eq. (22) if

$$-1 \leqslant 1 - 4\eta_j r \sin^2 \frac{m\pi}{2(n+1)} \leqslant 1$$

for each $j = 1, 2, \ldots, n_t$, where $n_t = T/\Delta t$. One sufficient condition for the stability of the scheme is

$$\eta_j r \leqslant \frac{1}{2}. \tag{32}$$

Substituting Eq. (29) for η_j into the above inequality we obtain

$$\eta_j r \leqslant \frac{r - 2r^2 \sin^2 \frac{\pi}{2(n+1)}}{1 - 4r^2 \sin^4 \frac{n\pi}{2(n+1)}}. \tag{33}$$

Due to

$$\sin^4 \frac{n\pi}{2(n+1)} - \sin^2 \frac{\pi}{2(n+1)} > 0, \quad \forall n \in \mathbb{N}, \tag{34}$$

from Eq. (33) we find that the range of r for stability is

$$r \leqslant r_{\max} = \frac{-1 + \sqrt{1 + 4\left[\sin^4 \frac{n\pi}{2(n+1)} - \sin^2 \frac{\pi}{2(n+1)}\right]}}{4\left[\sin^4 \frac{n\pi}{2(n+1)} - \sin^2 \frac{\pi}{2(n+1)}\right]}. \tag{35}$$

In Fig. 1, $r_{\max}$ is plotted with respect to n, of which we can see that the admissible range of r is smaller than 1/2 for the Euler method.

4. The backward heat conduction problems

4.1. Semi-discretization

In order to treat the one-dimensional backward heat conduction problems (1)–(3), let us consider the independent variable transformation $s = T - t$, reversing the time direction, such that one has

$$\frac{\partial u}{\partial s} = -v \frac{\partial^2 u}{\partial x^2}, \quad x \in D, \ 0 < s < T, \tag{36}$$

$$u(x, s) = u_B, \quad x \in \partial D, \tag{37}$$

$$u(x, 0) = u_F, \quad x \in D. \tag{38}$$

Here $u = u(x, s)$. In terms of the reverse time s it is a forward initial-boundary-value problem; however, the heat diffusion coefficient $-v$ is negative.

The semi-discretization of Eq. (36) is

$$\frac{\partial u_i(s)}{\partial s} = \frac{v}{(\Delta x)^2}[-u_{i+1}(s) + 2u_i(s) - u_{i-1}(s)]. \tag{39}$$

Due to the positive factor $2v/(\Delta x)^2$ preceding $u_i(s)$, any numerical integration scheme will blow up very soon. Therefore, let us further consider the dependent variables transformation

$$v_i(s) = e^{-as} u_i(s), \quad i = 1, \ldots, n, \tag{40}$$

where $a > 0$ is a contraction factor to be determined, such that the discretization (39) in terms of $v_i(s)$ is changed to

$$\begin{aligned} \frac{\partial v_i(s)}{\partial s} &= -a v_i(s) + \frac{v}{(\Delta x)^2}[-v_{i+1}(s) + 2v_i(s) - v_{i-1}(s)] \\ &= \left[\frac{2v}{(\Delta x)^2} - a\right] v_i(s) - \frac{v}{(\Delta x)^2}[v_{i+1}(s) + v_{i-1}(s)]. \end{aligned} \tag{41}$$

Clearly, we prefer to choose a such that $2v/(\Delta x)^2 - a \leqslant 0$ for numerical stability reasons. The stability analyses of the above equation by group preserving scheme is reported below. The discretized conditions of v and u at $s = 0$ are both the same, obtained by inserting the discretized $x_i = i\Delta x, i = 1, \ldots, n$, into Eq. (38). After $v_i(s)$ is integrated numerically, we can obtain $u_i(s) = e^{as} v_i(s)$.

4.2. Stability analysis

Employing the group preserving scheme to Eq. (41) we obtain

$$v_i^{j+1} = v_i^j + \eta_j r[2 - b] v_i^j - \eta_j r[v_{i+1}^j + v_{i-1}^j], \tag{42}$$

where

$$b = \frac{a(\Delta x)^2}{v}. \tag{43}$$

In the vector form as that done in Eq. (31), from Eq. (42) we have

$$\mathbf{v}^{j+1} = \mathbf{A}_j \mathbf{v}^j = [\mathbf{I}_n - \eta_j r(b\mathbf{I}_n + \mathbf{C})]\mathbf{v}^j, \tag{44}$$

where $\mathbf{v}^j = (v_1^j, v_2^j, \dots, v_n^j)^t$, the matrix $\mathbf{C}$ is still defined by Eq. (23), and $\mathbf{A}_j$ represents the new coefficient matrix at the time step t_j. The eigenvalues of $\mathbf{A}_j$ are found to be

$$1 - b\eta_j r + 4\eta_j r \sin^2 \frac{m\pi}{2(n+1)}, \quad m = 1, 2, \dots, n.$$

The scheme (42) is stable if

$$-1 \leqslant 1 - b\eta_j r + 4\eta_j r \sin^2 \frac{m\pi}{2(n+1)} \leqslant 1 \tag{45}$$

for each $j = 1, 2, \dots, n_s$, where $n_s = T/\Delta s$. One sufficient condition for the stability of this scheme is $b \geqslant 4$ and

$$\eta_j r \leqslant \frac{2}{b} < \frac{2}{b - 4\sin^2 \frac{m\pi}{2(n+1)}}. \tag{46}$$

The adaptive factor η_j can be written as

$$\eta_j = \frac{4\|\mathbf{v}^j\|^2 - 2r[(\mathbf{v}^j)^t\mathbf{C}\mathbf{v}^j + b\|\mathbf{v}^j\|^2]}{4\|\mathbf{v}^j\|^2 - r^2[(\mathbf{v}^j)^t\mathbf{C}^2\mathbf{v}^j + 2b(\mathbf{v}^j)^t\mathbf{C}\mathbf{v}^j + b^2\|\mathbf{v}^j\|^2]}, \tag{47}$$

upon inserting the vector fields $\mathbf{f}^j = -v\mathbf{C}\mathbf{v}^j/(\Delta x)^2 - bv\mathbf{v}^j/(\Delta x)^2$ into Eq. (16).

Let $\mathbf{n}^j = \mathbf{v}^j/\|\mathbf{v}^j\|$ be a unit vector, and Eq. (47) is changed to

$$\eta_j = \frac{4 - 2r[(\mathbf{n}^j)^t\mathbf{C}\mathbf{n}^j + b]}{4 - r^2[(\mathbf{n}^j)^t\mathbf{C}^2\mathbf{n}^j + 2b(\mathbf{n}^j)^t\mathbf{C}\mathbf{n}^j + b^2]}. \tag{48}$$

Due to Eqs. (27) and (28), the upper bound of η_j can be estimated as follows:

$$\eta_j \leqslant \frac{4 + 8r\sin^2 \frac{\pi}{2(n+1)} - 2br}{4 - 16r^2 \sin^4 \frac{n\pi}{2(n+1)} + 8br^2 \sin^2 \frac{\pi}{2(n+1)} - b^2r^2}. \tag{49}$$

Substituting Eq. (49) for η_j into the inequality (46) we obtain

$$\frac{4r + 8r^2\sin^2 \frac{\pi}{2(n+1)} - 2br^2}{4 - 16r^2 \sin^4 \frac{n\pi}{2(n+1)} + 8br^2 \sin^2 \frac{\pi}{2(n+1)} - b^2r^2} \leqslant \frac{2}{b}. \tag{50}$$

Therefore the range of r for stability is found to be

$$r \leqslant r_{\max} = \frac{-b + \sqrt{b^2 + 8\left[8\sin^4 \frac{n\pi}{2(n+1)} - 2b\sin^2 \frac{\pi}{2(n+1)}\right]}}{2\left[8\sin^4 \frac{n\pi}{2(n+1)} - 2b\sin^2 \frac{\pi}{2(n+1)}\right]}. \tag{51}$$

When $b = 4$ the above formula is equivalent to Eq. (35), and $r_{\max}$ was already plotted in Fig. 1 with respect to n. In the same figure we also plot the curves for $b = 4.5$ and $b = 5$. The stability range decreases when b increases. However, we should stress that the stability criterion just provides a sufficient condition, which does not mean that the numerical scheme with a smaller value of $b < 4$ will be unstable.

5. Numerical examples

5.1. Example one

Let us first consider the one-dimensional heat flow equation

$$u_t = vu_{xx}, \quad 0 < x < 2, \; 0 < t < T, \tag{52}$$

with the boundary conditions

$$u(0, t) = u(2, t) = 0,$$

and the initial condition

$$u(x, 0) = \begin{cases} 100x, & \text{for } 0 \leqslant x \leqslant 1, \\ 100(2 - x), & \text{for } 1 \leqslant x \leqslant 2. \end{cases}$$

The exact solution is given by

$$u(x, t) = 800 \sum_{k=0}^{\infty} \frac{1}{\pi^2(2k+1)^2} \cos \frac{(2k+1)\pi(x-1)}{2} \times \exp[-\pi^2 v(2k+1)^2 t/4]. \tag{53}$$

The numerical solution is subjected to the initial condition

$$u_i(0) = \begin{cases} 100i\Delta x, & \text{for } 0 \leqslant i\Delta x \leqslant 1, \\ 100(2 - i\Delta x), & \text{for } 1 \leqslant i\Delta x \leqslant 2. \end{cases} \tag{54}$$

The one-dimensional domain [0,2] is discretized by $n + 2$ points and i in u_i is numbered from 0 to $n + 1$. The two boundary conditions at the two end points are specified by $u_0(t) = u_{n+1}(t) = 0$. The error of numerical solution at point $x = 0.8$ is plotted in Fig. 2, and the error at time $T = 1$ is plotted in Fig. 2(b). For this computational example we have taken $v = 0.1$, $n = 100$ and $\Delta t = 0.001$ s. The exact solution is obtained from Eq. (54) by taking the sum of the first hundred terms, which guarantees the convergence of the series solution. The accuracy as can be seen is in the order of $O(\Delta t)$.

5.2. Example two

Let us then consider the one-dimensional heat flow equation

$$u_t = u_{xx}, \quad 0 < x < 1, \quad 0 < t < T, \tag{55}$$

with the boundary conditions

$$u(0, t) = 0, \quad u(1, t) = 1,$$

and the initial condition

$$u(x, 0) = \sin \pi x + x.$$

The exact solution is given by

$$u(x, t) = e^{-\pi^2 t} \sin \pi x + x. \tag{56}$$

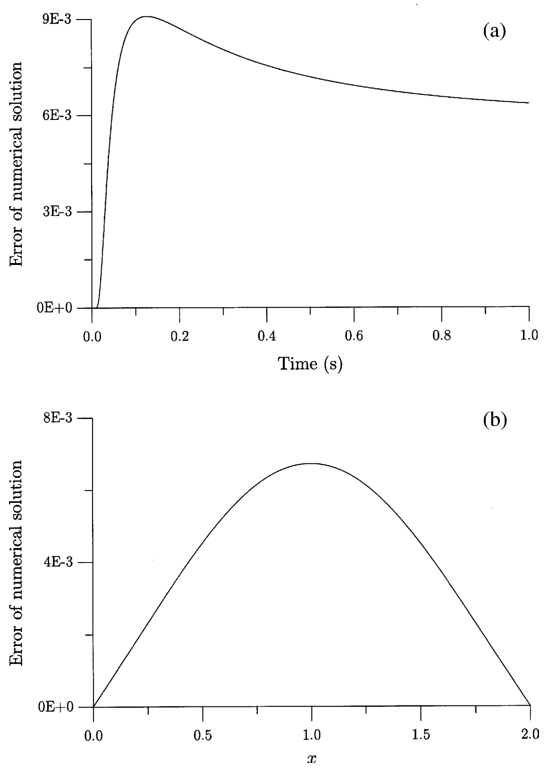

Fig. 2. The errors of numerical solutions for example one are plotted in (a) with respect to time at a fixed grid point $x = 0.8$, and in (b) with respect to x at the final time $T = 1$.

The numerical solution by group preserving scheme (GPS) is summarized in Table 1 to show the numerical values at point $x = 0.5$ for different times, where $n = 20$ and $\Delta t = 0.001$ s were used in our calculation. In the same table the Galerkin solutions given in [11] with $N = 2, 3$ orders are also included to compare with the exact solution (56) as well as with GPS solutions. It can be seen that GPS solutions are more accurate than that of the Galerkin solutions. Our scheme is easier to implement than that of the Galerkin method, which requires to do a lot of integrals before obtaining the N ordinary differential equations for the N variable coefficients.

Table 1
The comparison of numerical solutions with exact solution of example two

Time (s)	Galerkin ($N = 2$)	Galerkin ($N = 3$)	GPS	Exact
0.02	1.32611	1.32020	1.32083	1.32087
0.04	1.18389	1.17278	1.17373	1.17383
0.06	1.06757	1.05188	1.05296	1.05312
0.08	0.97242	0.95274	0.95382	0.95404
0.10	0.89461	0.87144	0.87243	0.87271
0.12	0.83096	0.80477	0.80563	0.80594
0.14	0.77890	0.75009	0.75080	0.75114
0.16	0.73632	0.70526	0.70580	0.70615
0.18	0.70150	0.66849	0.66886	0.66922
0.20	0.67301	0.63833	0.63856	0.63891

5.3. Example three

Let us consider the third example of one-dimensional backward heat flow equation

$$u_t = u_{xx}, \quad -\pi < x < \pi, \;\; T > t > 0, \tag{57}$$

with the boundary conditions

$$u(-\pi, t) = u(\pi, t) = 0,$$

and the final time condition

$$u(x, T) = e^{-\alpha^2 T} \sin \alpha x.$$

The exact solution is given by

$$u(x, t) = e^{-\alpha^2 t} \sin \alpha x, \tag{58}$$

where $\alpha \in \mathbb{N}$ is a positive integer.

As remarked in Section 1 this problem is ill-posed. However, we can demonstrate it further by considering the L^2-norms of u and its final data:

$$\begin{aligned} \|u(x,t)\|_{L^2}^2 &= \int_0^T \int_{-\pi}^{\pi} (e^{-\alpha^2 t} \sin \alpha x)^2 \, dx \, dt \\ &= \frac{1}{2\alpha^2}(e^{2\alpha^2 T} - 1) \int_{-\pi}^{\pi} (e^{-\alpha^2 T} \sin \alpha x)^2 \, dx. \end{aligned} \tag{59}$$

Since, for any $C > 0$ there exists $\alpha \in \mathbb{N}$ such that $\sqrt{e^{2\alpha^2 T} - 1}/(\sqrt{2}\alpha) > C$, an inequality $\|u(x,t)\|_{L^2} > C\|u_F\|_{L^2}$ holds for any $C > 0$. This means that the solution does not depend on the final data continuously. Therefore, the backward heat conduction problem is unstable for given final data with respect to the L^2-norm. The larger α is, the worse the final data dependence of the solution is. In other words, the problem is more ill-posed when α is larger. While we said that the problem with $\alpha \geqslant 3$ is strongly ill-posed, those with $\alpha < 3$ may be said to be moderately or weakly ill-posed.

In Fig. 3 we show the numerical results compared with the exact solution (58) at time $t = 0$ for three cases $\alpha = 1, 2, 3$. $T = 1$ s was used in this comparison, the grid length is taken to be $\Delta x = \pi/10$ for the first and second cases and $\Delta x = \pi/13$ for the last case, the step size of s is taken to be $\Delta s = 0.1$ s, and $b = 2$ was chosen. For the first case the numerical error is very small in the order $O(10^{-3})$, and for the second case the numerical error increased to the order $O(10^{-2})$. For the last case it can be seen that the error is rather large in the order of $O(10^{-1})$, which is due to the very small final data in the order $O(10^{-4})$ when compared with the desired initial data

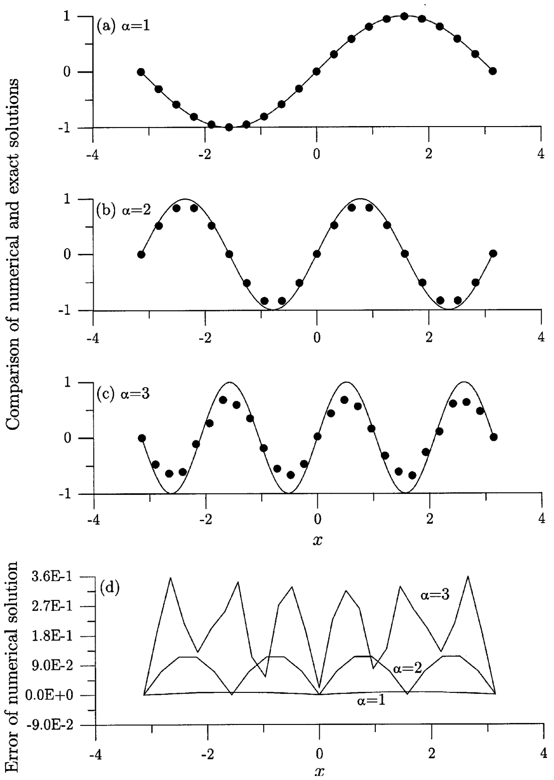

Fig. 3. The comparison of exact solutions and numerical solutions for example three of one-dimensional backward problem are made in (a) with the case $\alpha = 1$, (b) with the case $\alpha = 2$, and (c) with the case $\alpha = 3$. The errors of numerical solutions are plotted in (d) with respect to x at the initial time $t = 0$.

$\sin \alpha x$ of order $O(1)$ to be retrieved, and is also due to the accumulation of round-off error in the computation. It should be reminded that the contraction factor $a = b/(\Delta x)^2$ was selected according to two criteria: numerical stability and to avoid a very large value of $\exp(aT)$. Since b is an important factor, we compare the numerical errors at different grid points of this example with $\alpha = 1$ for different b's in Table 2. The numerical errors at the mid grid point, i.e. $x = 0$, are all zero. It can be seen that the three $b = 1.5, 2, 2.5$ give little influence on the numerical errors. When $b = 3$ the numerical errors at the first three grid points are smaller than the others, but the numerical errors at the last three grid points are larger than the others. Upon using $b = 4$ we require larger Δx to avoid larger a. For example, by using $\Delta x = 2\pi/15$ and $\Delta s = 0.05$ s on this case, the numerical errors are increased to the order $O(10^{-2})$ at several grid points. Under this condition the enlarged factor $\exp(a) = \exp(22.8)$ is too large to increase the accuracy.

5.4. Example four

Let us consider the final example of two-dimensional backward heat flow equation

$$u_t = u_{xx} + u_{yy}, \quad -\pi < x < \pi, \ -\pi < y < \pi, \ T > t > 0, \tag{60}$$

with the boundary conditions

$$u(-\pi, y, t) = u(\pi, y, t) = u(x, -\pi, t) = u(x, \pi, t) = 0, \tag{61}$$

and the final time condition

$$u(x, y, T) = e^{-2\alpha^2 T} \sin \alpha x \sin \alpha y. \tag{62}$$

The exact solution is given by

$$u(x, y, t) = e^{-2\alpha^2 t} \sin \alpha x \sin \alpha y, \tag{63}$$

where $\alpha \in \mathbb{N}$ is a positive integer.

Upon considering the independent variable transformation $s = T - t$, Eqs. (60)–(62) become

$$u_s = -u_{xx} - u_{yy}, \quad -\pi < x < \pi, \ -\pi < y < \pi, \ 0 < s < T, \tag{64}$$

$$u(-\pi, y, s) = u(\pi, y, s) = u(x, -\pi, s) = u(x, \pi, s) = 0, \tag{65}$$

$$u(x, y, 0) = e^{-2\alpha^2 T} \sin \alpha x \sin \alpha y. \tag{66}$$

Here u is a function with $u = u(x, y, s)$. In terms of s it is a forward initial-boundary-value problem. The semi-discretization of Eq. (64) is

Table 2
The comparison of numerical errors with different b's of example three with $\alpha = 1$

$x = -\pi + k\pi/10$	$b = 1.5$	$b = 2$	$b = 2.5$	$b = 3$
$k = 3$	0.6605×10^{-2}	0.6602×10^{-2}	0.6631×10^{-2}	0.4805×10^{-2}
$k = 5$	0.8164×10^{-2}	0.8160×10^{-2}	0.8187×10^{-2}	0.5970×10^{-2}
$k = 9$	0.2523×10^{-2}	0.2522×10^{-2}	0.2515×10^{-2}	0.1996×10^{-2}
$k = 14$	0.7765×10^{-2}	0.7768×10^{-2}	0.7753×10^{-2}	0.9771×10^{-2}
$k = 16$	0.7765×10^{-2}	0.7768×10^{-2}	0.7737×10^{-2}	0.9884×10^{-2}
$k = 18$	0.4799×10^{-2}	0.4801×10^{-2}	0.4780×10^{-2}	0.6102×10^{-2}

$$\frac{\partial u_{i,j}(s)}{\partial s} = \frac{1}{(\Delta x)^2}[-u_{i+1,j}(s) + 2u_{i,j}(s) - u_{i-1,j}(s)] + \frac{1}{(\Delta y)^2}[-u_{i,j+1}(s) + 2u_{i,j}(s) - u_{i,j-1}(s)]. \quad (67)$$

where $u_{i,j}(s) = u(i\Delta x, j\Delta y, s)$. Then, let us consider the dependent variables transformation

$$v_{i,j}(s) = e^{-as}u_{i,j}(s), \quad i = 1,\ldots,n, \quad j = 1,\ldots,n, \quad (68)$$

such that the discretization (67) in terms of $v_{i,j}(s)$ is changed to

$$\frac{\partial v_{i,j}(s)}{\partial s} = \left[\frac{2}{(\Delta x)^2} + \frac{2}{(\Delta y)^2} - a\right] v_{i,j}(s) - \frac{1}{(\Delta x)^2} \times [v_{i+1,j}(s) + v_{i-1,j}(s)] - \frac{1}{(\Delta y)^2}[v_{i,j+1}(s) + v_{i,j-1}(s)]. \quad (69)$$

Clearly, we prefer to choose a such that $2/(\Delta x)^2 + 2/(\Delta y)^2 - a \leqslant 0$ for numerical stability reasons.

In Fig. 4 we show the errors of numerical solutions by taking the absolute of the differences with respect to the exact solution (63) at time $t = 0$ for one case $\alpha = 1$.

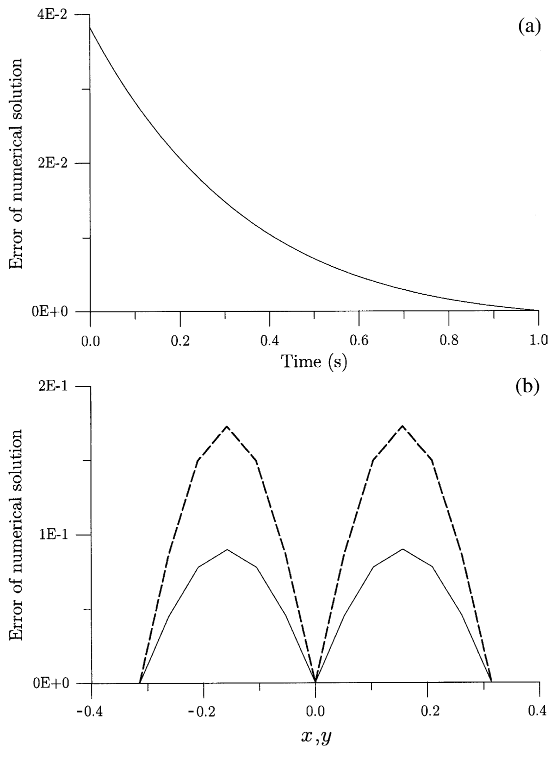

Fig. 4. The errors of numerical solutions for example four of two-dimensional backward problem are plotted in (a) with respect to time at a fixed grid point $(\pi/2, 2\pi/3)$, and in (b) at the initial time with respect to y and fixed $x = \pi/2$ (- - -), and with respect to x and fixed $y = 2\pi/3$ (—).

$T = 1$ s was used in this comparison, the grid lengths are taken to be $\Delta x = \Delta y = \pi/6$, the step size of s is taken to be $\Delta s = 0.01$ s, and $a = 4/(\Delta x)^2 + 4/(\Delta y)^2$ was chosen for stability. In Fig. 4(a) the numerical error is plotted with respect to time at the grid point $(x, y) = (\pi/2, 2\pi/3)$. At the same time, the numerical errors at zero time are plotted in Fig. 4(b) with a dashed line for fixed $x = \pi/2$ and varied y in the range $[-\pi, \pi]$, and with a solid line for fixed $y = 2\pi/3$ and varied x in the range $[-\pi, \pi]$.

6. Conclusions

The heat conduction problems are calculated by the formulation with a semi-discretization of heat conducting equations in conjuction with the group preserving numerical integration scheme. As well known, in the backward numerical integration of the heat conduction equations, a simple employment of the finite difference or finite element method with negative time steps is numerically unstable. In this paper we are concerned with this numerical integration problem, in which the key points were the consideration of two transformations: $s = T - t$ and $v = \exp[-as]u$. The first transformation renders the backward problem to become a forward problem, and then the second transformation stabilizes it to a semi-discretized system of ordinary differential equations. The factor a is very important by subjecting certain constraints. The ranges of a and the stability index r of the group preserving scheme, which applied on the ordinary differential equations at the interior grid points, were analyzed and given. Four numerical examples (two of forward problems and the other two of backward problems) were worked out, which show that our numerical integration methods are applicable to the forward problems and also to the backward problems with weak or moderate ill-posedness.

References

[1] W.E. Williams, Partial Differential Equations, Oxford University Press, New York, 1980.

[2] H. Han, D.B. Ingham, Y. Yuan, The boundary element method for the solution of the backward heat conduction equation, J. Comp. Phys. 116 (1995) 292–299.

[3] N.S. Mera, L. Elliott, D.B. Ingham, D. Lesnic, An iterative boundary element method for solving the one-dimensional backward heat conduction problem, Int. J. Heat Mass Transfer 44 (2001) 1937–1946.

[4] N.S. Mera, L. Elliott, D.B. Ingham, An inversion method with decreasing regularization for the backward heat conduction problem, Numer. Heat Transfer B 42 (2002) 215–230.

[5] S.M. Kirkup, M. Wadsworth, Solution of inverse diffusion problems by operator-splitting methods, Appl. Math. Modell. 26 (2002) 1003–1018.

[6] K. Iijima, Numerical solution of backward heat conduction problems by a high-order lattice-free finite difference method, J. Chin. Inst. Engrs. submitted for publication.
[7] L.D. Chiwiacowsky, H.F. de Campos Velho, Different approaches for the solution of a backward heat conduction problem, Inv. Probl. Eng. 11 (2003) 471–494.
[8] R.D. Richtmyer, K.W. Morton, Difference Methods for Initial-Value Problems, second ed., Interscience Publishers, New York, 1967.
[9] C.-S. Liu, Cone of non-linear dynamical system and group preserving schemes, Int. J. Non-Linear Mech. 36 (2001) 1047–1068.
[10] W.E. Schiesser, The Numerical Method of Lines: Integration of Partial Differential Equations, Academic Press, San Diego, 1991.
[11] C.A.J. Fletcher, Computational Galerkin Methods, Springer-Verlag, New York, 1984.